Computer Simulation of Twin Formation during the Displacive $c \rightarrow t'$ Phase Transformation in the Zirconia–Yttria System

Danan Fan[*] and Long-Qing Chen[*]

Department of Materials Science and Engineering, The Pennsylvania State University,
University Park, Pennsylvania 16802

The kinetics of the displacive cubic-to-tetragonal ($c \rightarrow t'$) phase transformation and the evolution of twin structure of Y_2O_3–ZrO_2 systems were investigated by employing the time-dependent Ginzburg–Landau equations, in which the displacive modes were described by nonconserved order parameters. The original elasticity theory of Khachaturyan, in a sharp-interface description for an arbitrary distribution of second-phase precipitates in a matrix, was reformulated in the spirit of the diffuse interface theory of Cahn and Hilliard for interphase boundaries. The influence of thermodynamic conditions, clamped or stress-free, on microstructure evolution was studied. Our computer simulation showed that, even though the thermodynamic equilibrium is the single domain under a stress-free condition, the twin structure can form during a kinetic path of the phase transformation, and it is the clamped condition which results in the formation of stable twins.

I. Introduction

EXTENSIVE research has been devoted in the last decade to the development of ZrO_2-based ceramics,[1] because of the considerable potential of these ceramics in structural applications. Many experimental results and thermodynamic modeling of the cubic (c) → tetragonal (t) transformation in Y_2O_3–ZrO_2 systems have been reported.[1,2] It has been shown that, if a c-phase at a high temperature is rapidly quenched to the low-temperature two-phase ($c + t$) region of the phase diagram, precipitation of the t-phase is preceded by a diffusionless phase transformation, resulting in the formation of an intermediate t' single phase. A characteristic feature of the t'-phase is that it has the same composition as the original c-phase. Microstructurally, it is characterized by the presence of antiphase-domain boundaries (APBs)[3] within a single orientation domain and twins formed by different orientation variants.[4]

In a $c \rightarrow t$ transformation, the number of different orientation variants dictated by the crystal symmetry is three, with the tetragonal axes along the crystallographic directions [100], [010], and [001] of the parent cubic phase. Thermodynamically, the existence of more than one orientation variant provides a configurational freedom to reduce the total elastic energy arising from a crystal lattice misfit at the c/t phase boundaries and at the boundaries between different t-phase orientation variants. In the case of a two-phase mixture of c- and t-phases, twin-related "sandwiches" of different orientation domains of the t-phase can be organized into plates in such a way that they eliminate the volume-dependent part of the elastic energy and the resulting elastic energy is only proportional to the interfacial area. If the transformation product is a t single phase, the final

equilibrium state depends on the stress conditions. For example, when a single-crystal c-phase with free surfaces transforms to a single t-phase, the equilibrium state is expected to be a single-domain t-phase. However, if a c-phase cannot change its volume during a transformation, e.g., a c-phase grain constrained in a polycrystalline assembly, it can be shown that the equilibrium state under this clamped condition is the twin structure composed of different orientation variants of the t-phase.

While it is possible to predict the final equilibrium state under a specified condition using thermodynamics, the detailed temporal evolution of microstructures during the entire process of a $c \rightarrow t$ transformation can only be elucidated by a kinetic computer simulation.

The earliest discussion of the elastic strain energy effect on microstructures in a kinetics context is that due to Cahn for spinodal decomposition.[5] Recently, there have been extensive computer simulation studies on the strain-induced morphological transformations for the simple case of decomposition of a cubic phase into two cubic phases with different compositions using the continuum TDGL model,[6] microscopic diffusion equations,[7,8] and boundary integral equations.[9,10] The shape evolution of a single tetragonal precipitate in a cubic matrix was investigated by using the continuum model[11] and boundary integral equations.[12] The kinetics of tweed and twin formation during a disorder–order transition (cubic → tetragonal) in substitutional solution[13] and in interstitial solutions (tetragonal → orthorhombic)[14,15] were studied using microscopic models.

In this paper, we report our computer simulation studies of the temporal and spatial evolution of microstructures during the *displacive* $c \rightarrow t'$ transformation in the Y_2O_3–ZrO_2 system by using the continuum time-dependent Ginzburg–Landau (TDGL) kinetic model.[11] In particular, we investigated the temporal microstructure evolution during a $c \rightarrow t'$ transformation under different thermodynamic conditions, stress-free or clamped. In order to incorporate the elastic energy into the continuum TDGL model, the original sharp-interface linear elasticity theory of Khachaturyan[16,17] was rederived using the diffuse interface theory of Cahn and Hilliard[18] and Allen and Cahn.[19] The effect of elastic energy on the phase diagram is briefly discussed. The detailed kinetics of decomposition of the t' phase into a two-phase mixture of equilibrium c- and t-phases will be discussed in a future publication.

II. The TDGL Model

In order to describe a structural transformation with symmetry changes, it is necessary to introduce order parameter fields or phase-fields, $\eta_i(\mathbf{r})$ ($i = 1, 2, 3, \ldots, \nu$, where ν is the number of different orientation domains of the product phase dictated by the crystallographic relationship of the product and parent phases), to characterize the symmetry difference between the parent and product phases. Physically, these field variables describe the amplitudes of displacive modes in the case of a displacive transformation. For a mixture of two phases with different compositions, a continuous field of composition, $c(\mathbf{r})$, also needs to be defined. The temporal and spatial evolution of these order parameter fields and composition fields toward

equilibrium in a quenched system may be described by the Ginzburg–Landau (Allen–Cahn)[18,20] and Cahn–Hilliard[19] equations:

$$\frac{\partial \eta_i(\mathbf{r},t)}{\partial t} = -L\frac{\delta F}{\delta \eta_i(\mathbf{r},t)} \qquad i = 1, \ldots, \nu \qquad (1a)$$

$$\frac{\partial c(\mathbf{r},t)}{\partial t} = M\nabla^2\frac{\partial F}{\delta c(\mathbf{r},t)} \qquad (1b)$$

in which L and M are kinetic coefficients which characterize the interphase interface mobility and atomic diffusivity, and F is the total free energy expressed in the unit of $k_B T$, where k_B is the Boltzmann constant and T is the temperature.

In a structural transformation, the total nonequilibrium free energy F is the sum of the "chemical" free energy F_c and the strain energy E. The chemical free energy is associated with the finite-range interatomic interaction and, according to the diffuse interface theory by Cahn and Hilliard,[18] it can be written as

$$F_c = \int_v\left[\frac{1}{2}\alpha|\nabla_c|^2 + \frac{1}{2}\beta\left(\sum_{i=1}^{\nu}|\nabla\eta_i|^2\right) + f(c,\eta_1,\eta_2\ldots,\eta_\nu)\right]dv \qquad (2)$$

where α and β are gradient energy coefficients for concentration and order parameters, respectively, and f is the local free energy density, which is a function of composition and order parameter fields.

III. Diffuse Interface Formulation of Khachaturyan's Elasticity Theory

An expression for strain energy induced by an arbitary distribution of coherent second-phase particles was developed by Khachaturyan *et al.*[16,17] and has been successfully applied to different phase transformations.[7,8,11] In that expression, a sharp interface between a second-phase particle and matrix was assumed and the distribution of second-phase particles was described by the so-called shape function,

$$\theta_p(\mathbf{r}) = \begin{cases} 1 & \text{inside a second-phase particle of kind } p \\ 0 & \text{otherwise} \end{cases}$$

It is schematically shown in Fig. 1(a) as a step function in one dimension. It has the properties

$$\theta_p(\mathbf{r})\,\theta_p(\mathbf{r}) = \theta_p(\mathbf{r}) \qquad (3)$$

$$\theta_p(\mathbf{r})\,\theta_q(\mathbf{r}) = 0 \qquad p \neq q \qquad (4)$$

and

$$\int_v \theta(\mathbf{r})\,dv = V_p \qquad (5)$$

where V_p is the total volume of second-phase particles of kind p. The local stress-free transformation strain is given by

$$\varepsilon_{ij}^0(\mathbf{r}) = \sum_{p=1}^{\nu} \theta(\mathbf{r})\varepsilon_{ij}^0(p) \qquad (6)$$

However, if $\theta(\mathbf{r})$ is a continuous field, the relations (3), (4),

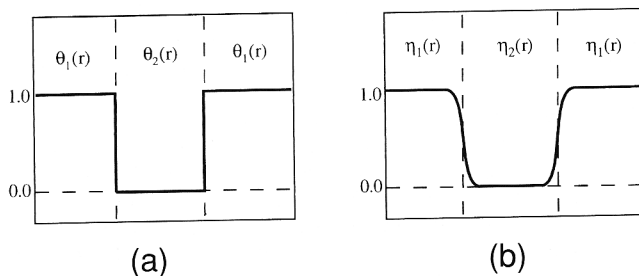and (5) do not hold anymore. For example, during a $c \to t$ phase transformation, the local stress-free transformation strain $\varepsilon_{ij}^0(\mathbf{r})$ is related to a continuous field through

$$\varepsilon_{ij}^0(\mathbf{r}) = \sum_{p=1}^{q} \varepsilon_{ij}^0(p)\eta_p^2(\mathbf{r}) \qquad (7)$$

where $\varepsilon_{ij}^0(p)$ and $\eta_p(\mathbf{r})$ are the proportionality constants and local order parameter field for a particular variant p, respectively. For comparison with the sharp-interface description, the local order parameter field is schematically shown in Fig. 1(b) in one dimension.

We assume that the c-phase and t-phase have the same elastic moduli. If elastic displacements were not allowed during a phase transformation, there would be an elastic energy increase given by

$$\begin{aligned}
E_1 &= \frac{1}{2}\int_v \lambda_{ijkl}\varepsilon_{ij}^0(\mathbf{r})\varepsilon_{kl}^0(\mathbf{r})\,dv \\
&= \frac{1}{2}\int_v \lambda_{ijkl}\left[\sum_{p=1}^{3}\varepsilon_{ij}^0(p)\eta_p^2(\mathbf{r})\right]\left[\sum_{q=1}^{3}\varepsilon_{kl}^0(q)\eta_q^2(\mathbf{r})\right]dv \\
&\cong \frac{1}{2}\int_v \lambda_{ijkl}\sum_{p=1}^{3}\varepsilon_{ij}^0(p)\varepsilon_{kl}^0(p)\eta_p^4(\mathbf{r})\,dv
\end{aligned} \qquad (8)$$

where λ_{ijkl} is the elastic modulus tensor, the integration being taken over the system volume v. The cross terms, $\eta_p^2(\mathbf{r})\eta_q^2(\mathbf{r})$, are not zero only at boundaries between orientation domains p and q, and therefore are neglected in Eq. (8).

The elastic energy can be partially relaxed by introducing elastic strains. Following Khachaturyan,[17] the total relaxation energy E_{relax} has the form

$$E_{relax} = \int_v\left[-\sigma_{ij}^0(\mathbf{r})\varepsilon_{ij}(\mathbf{r}) + \frac{1}{2}\lambda_{ijkl}\varepsilon_{ij}(\mathbf{r})\varepsilon_{kl}(\mathbf{r})\right]dv \qquad (9)$$

where $\sigma_{ij}^0(\mathbf{r}) = \sum_{p=1}^{3}\sigma_{ij}^0(p)\eta_p^2(\mathbf{r})$ and $\sigma_{ij}^0(p) = \lambda_{ijkl}\varepsilon_{kl}^0(p)$. The elastic strain field, $\varepsilon_{ij}(\mathbf{r})$, can be written as the sum of homogeneous and heterogeneous strains:

$$\varepsilon_{ij}^0(\mathbf{r}) = \bar{\varepsilon}_{ij} + \delta\varepsilon_{ij}(\mathbf{r}) \qquad (10)$$

where the homogeneous strain $\bar{\varepsilon}_{ij}$ is defined so that

$$\int_v \delta\varepsilon_{ij}(\mathbf{r})\,dv = 0 \qquad (11)$$

The strain $\bar{\varepsilon}_{ij}$ corresponds to the uniform macroscopic strain which determines the macroscopic shape deformation of a crystal. The heterogeneous strain $\delta\varepsilon_{ij}(\mathbf{r})$ does not produce any macroscopic effect.[17] Therefore, the total relaxation energy can also be separated into a sum of two terms: E^{hom} and E^{het}, where E^{hom} is the relaxation of elastic energy related to the homogeneous strain and E^{het} is the relaxation of elastic energy related to heterogeneous strain. Substituting (10) into (9) and using the condition (11) yield

$$E^{hom} = -\int_v \sum_{p=1}^{3}\sigma_{ij}^0(p)\eta_p^2(\mathbf{r})\,dv\,\bar{\varepsilon}_{ij} + \frac{V}{2}\lambda_{ijkl}\bar{\varepsilon}_{ij}\bar{\varepsilon}_{kl} \qquad (12a)$$

$$E^{het} = \int_v\left[-\sum_{p=1}^{3}\sigma_{ij}^0(p)\eta_p^2(\mathbf{r})\delta\varepsilon_{ij} + \frac{1}{2}\lambda_{ijkl}\delta\varepsilon_{ij}\delta\varepsilon_{kl}\right]dv \qquad (12b)$$

A system reaches mechanical equilibrium when the relaxation energies (12a) and (12b) are minimized with respect to the homogeneous strain and local displacements, respectively, i.e.,

$$\frac{\partial E_{relax}}{\partial \bar{\varepsilon}_{ij}} = 0 \qquad (13)$$

$$\frac{\partial E_{relax}}{\partial u_i(\mathbf{r})} = 0 \qquad (14)$$

where the displacement, $u_i(\mathbf{r})$ is related to heterogeneous strain by[17]

Fig. 1. Schematic shape function in one dimension. (a) Sharp interface; (b) local order parameter field with a diffuse interface.

$$\delta\varepsilon_{ij} = \frac{1}{2}\left(\frac{\partial u_i}{\partial r_j} + \frac{\partial u_j}{\partial r_i}\right) \tag{15}$$

The relaxation energies corresponding to the equilibrium homogeneous strain and equilibrium local displacements are given by

$$E^{hom} = -\frac{1}{2V}\sum_{p=1}^{3}\sum_{q=1}^{3}\lambda_{ijkl}\varepsilon_{ij}^{0}(p)\varepsilon_{kl}^{0}(q)\int_{v}\eta_p^2(\mathbf{r})\,d^3r\int_{v'}\eta_q^2(\mathbf{r'})\,d^3r' \tag{16}$$

$$E^{het} = -\frac{1}{2}\sum_{p=1}^{3}\sum_{q=1}^{3}\int\frac{d^3k}{(2\pi)^3}[n_i\sigma_{ij}^0(p)\Omega_{jk}(\mathbf{n})\sigma_{kl}^0(q)n_l]$$
$$\{\eta_p(\mathbf{r})^2\}_k\{\eta_q(\mathbf{r})^2\}_{\mathbf{k}}^{*} \tag{17}$$

where $\mathbf{k}$ is a wave-vector, $n_i = k_i/k$ is the ith component of a unit vector parallel to $\mathbf{k}$, $\Omega_{jk}(\mathbf{n})$ is a Green function matrix[17] reciprocal to $\Omega_{jk}^{-1} = \lambda_{ijkl}n_in_l$, and

$$\{\eta_p^2(\mathbf{r})\}\mathbf{k} = \int_{v}\eta_p^2(\mathbf{r})\exp(-i\mathbf{k}\cdot\mathbf{r})\,d^3r \tag{18}$$

$\{\eta_q(\mathbf{r})^2\}_{\mathbf{k}}^{*}$ is the complex conjugate of $\{\eta_q(\mathbf{r})^2\}_k$. The singular branching point $\mathbf{k} = 0$ is excluded from the integration in Eq. (17).

Therefore, the total elastic energy is given by

$$E = E_1 + E^{hom} + E^{het} \tag{19}$$

IV. Model for the Y_2O_3–ZrO_2 System

The $c \to t'$ phase transformation in Y_2O_3–ZrO_2 is treated as a first-order transition. The local specific chemical free energy at a given temperature is approximated by the free energy polynomial:

$$f(c,\eta_1,\eta_2,\eta_3) = \frac{1}{2}A(c - c_1)^2 + \frac{1}{2}B(c - c_2)\left(\sum_{i=1}^{3}\eta_i^2\right)$$
$$- \frac{1}{4}D\left(\sum_{i=1}^{3}\eta_i^4\right) + \frac{1}{6}G\left(\sum_{i=1}^{3}\eta_i^6\right)$$
$$+ U\left(\sum_{i\neq j}\eta_i^2\eta_j^2\right) + V\left(\sum_{i\neq j\neq k}\eta_i^4[\eta_j^2 + \eta_k^2]\right)$$
$$+ W(\eta_1^2\eta_2^2\eta_3^2) \tag{20}$$

where A, B, D, G, U, V, and W are positive constants, and c_1 is determined by the equilibrium composition of the cubic phase and c_2 is a constant beyond which the cubic phase is unstable. It is emphasized that our main interest is in the dynamics of a quenched system well below the phase transformation temperature. The exact form of the free energy function is not important as long as it has the cubic symmetry. The most important requirement is that it provides the proper phase diagram. Therefore, this free energy function can be viewed as an approximation to the actual free energies of c- and t-phases.

Equation (20) defines a hypersurface of the chemical free energy in a 4-dimensional phase space formed by c and the three order parameters η_i. By minimizing the free energy with respect to a given order parameter η_i at a given c, and under the condition that all other order parameters are zero, we can express the order parameter as a function of composition c and hence express the free energy as a function of c only. In Eq. (20), constants are chosen to provide the free-energy topology required for the Y_2O_3–ZrO_2 system in the two-phase region. In this work those constants are chosen as $A = 2.0$, $B = 1.1$, $D = 0.1$, $G = 1.5$, $U = 2.0$, and $V = W = 1.0$, which provide equilibrium compositions $c_{tet} = 0.024$ and $c_{cub} = 0.081$ close to

the equilibrium compositions of Y_2O_3–ZrO_2 at 1500°C.[1,4] The free energies for the c- and t-phases are shown in Fig. 2.

For the $c \to t'$ phase transformation, $\varepsilon_{ij}^0(p)$ can be written as

$$\varepsilon_{ij}^0(1) = \begin{bmatrix} \varepsilon_{33}^0 & 0 & 0 \\ 0 & \varepsilon_{11}^0 & 0 \\ 0 & 0 & \varepsilon_{11}^0 \end{bmatrix},\ \varepsilon_{ij}^0(2) = \begin{bmatrix} \varepsilon_{11}^0 & 0 & 0 \\ 0 & \varepsilon_{33}^0 & 0 \\ 0 & 0 & \varepsilon_{11}^0 \end{bmatrix},$$
$$\varepsilon_{ij}^0(3) = \begin{bmatrix} \varepsilon_{11}^0 & 0 & 0 \\ 0 & \varepsilon_{11}^0 & 0 \\ 0 & 0 & \varepsilon_{33}^0 \end{bmatrix} \tag{21}$$

where $\varepsilon_{11}^0 = (a_t - a_c)/a_c$, $\varepsilon_{33}^0 = (c_t - a_c)/a_c$. a_c is the lattice parameter of c-ZrO_2, and a_t and c_t are the lattice parameters of t-ZrO_2.

V. Computer Simulation Results

Because of the extensive computation involved in a three-dimensional (3D) kinetic study, we employed a two dimensional (2D) system which can be viewed as the projection from 3D system. In this case, $v = 2$ in previous equations and $\varepsilon_{ij}^0(\mathbf{r})$ is a plain strain. In the computer simulation, the kinetic equations are discretized by using a 256 × 256 grid with periodic boundary conditions along both directions.

The experimental data for the elastic constants of Y_2O_3–ZrO_2 are given as $c_{11} = 3.94 \times 10^{11}$ Pa, $c_{12} = 0.91 \times 10^{11}$ Pa, and $c_{44} = 0.56 \times 10^{11}$ Pa in Ref. 21; and lattice parameters, $a_c = 5.128$ Å, $a_t = 5.090$ Å, and $c_t = 5.180$ Å, are chosen from Ref. 1. All the energies involved in the numerical calculation are measured in units of $k_BT \sim 2 \times 10^8$ J/m^3. Reduced time t^* is used in the simulation, which is defined as $t^* = t/t_0$, $t_0 = (Lk_BT)^{-1}$.

The overall average composition, c, is chosen to be 0.056 (mole fraction). The initial condition is a homogeneous c-phase in which all values for the order parameter fields are zero. The cubic phase is then quenched to a temperature below the absolute instability line of the c-phase with respect to the transformation to the t'-phase, usually referred to as the T-line. In order to initiate the kinetics, however, random perturbations to the order parameters fields are introduced. Since our main interest is the diffusionless transformation from a single c-phase to a single t'-phase, we only solved the kinetic equations for the order parameter fields while keeping the composition homogeneous. Since we do not have the information about the antiphase domain boundary energy in the t'-phase, we rather arbitrarily assumed the gradient coefficient β in Eq. (3) to be 3.0.
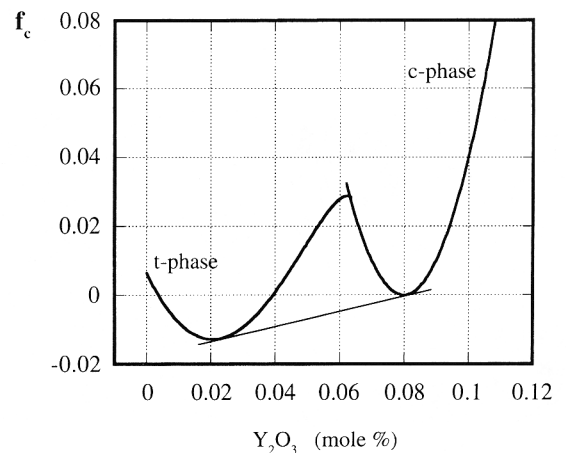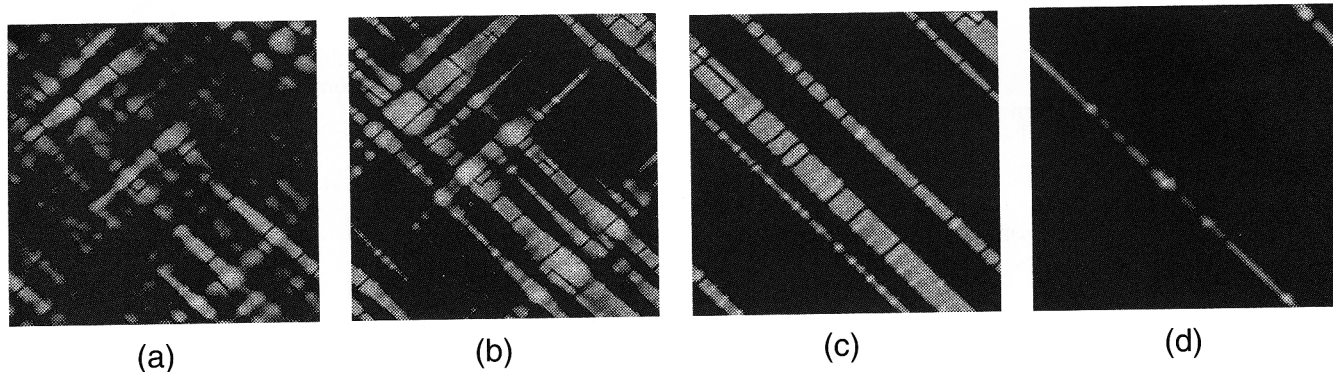

Fig. 2. Specific free-energy vs composition curves for both the cubic and tetragonal phases calculated according to Eq. (20) with $A = 2.0$, $B = 1.1$, $D = 0.1$, $G = 1.5$, $U = 2.0$, and $W = V = 1.0$.

Fig. 3. (a–d) Temporal evolution of $\eta_1(\mathbf{r})$ orientation field during a phase transformation with the total elastic energy $E = E_1 + E^{hom} + E^{het}$. (a–d) correspond to $t^* = 0.2, 0.4, 1.0,$ and 3.0, respectively (see text for the definition of t^*).

(1) The Stress-Free Condition

The elastic strain energy under the stress-free condition contains both the homogeneous and heterogeneous strain relaxation. This means the macroscopic shape deformation of a crystal will occur during transformation and the crystal is stress-free on its surface. The morphological evolution from the initial c-phase to the t'-phase and subsequent t'-domain coarsening is shown in Fig. 3. In the figure, the "gray levels" represent different magnitudes of one order parameter of the two orientation variants. A completely white color represents the highest square value of that order parameter, and a completely dark means that the order parameter is about zero. This representation corresponds to dark-field transmission electron micrographs using a reflection from one of the orientation variants.

Figure 3(a–d) is the temporal evolution of $\eta_1(\mathbf{r})$ field. From Figs. 3(a) and (b) it can be seen that the initial stage of transformation consists of growth of two order parameters at different locations as well as an increase in the domain size. The two orientation domains preferentially align along $\{1\,1\}$ planes, forming the so-called "tweed" structure. This tweed structure coarsens and develops into a twin structure (Fig. 3(c)) as time increases, with the amount of one orientation variant significantly more than the other. This twin structure is unstable and finally the $\eta_1(\mathbf{r})$ orientation variant will disappear (Fig. 3(d)). As a result, a single domain of $\eta_2(\mathbf{r})$ with antiphase domain boundaries is formed.

(2) The Clamped Condition

Under the clamped condition, the homogeneous strain relaxation is prohibited and hence the E^{hom} term is excluded from total elastic energy in the calculation. Since the elastic energy term, E_1, depends only on the relative volume fraction of the tetragonal phase, i.e., it is configurationally independent, we may also ignore the E_1 term. The morphology evolution after excluding E_1 and E^{hom} from the total elastic energy is shown in Fig. 4. By comparing Fig. 4 with Fig. 3, the structure similarity is obvious. It turns out that both $\eta_1(\mathbf{r})$ and $\eta_2(\mathbf{r})$ variants are stable, and a stable twin structure is formed after excluding E_1 and E^{hom} from the total elastic energy (Fig. 4(d)). The final microstructure contains both orientation domains comprising the twins with the twin boundary being the $(1\,1)$ plane. Many antiphase domain boundaries exist within the domains. The microstructure shown in Fig. 4(d) agrees well with the twin microstructure observed in the Y_2O_3–ZrO_2 system (Fig. 5).[4]

VI. Discussion

From the above computer simulation results, it is clear that the morphological evolution during a $c \rightarrow t'$ transformation follows

$$c \rightarrow \text{tweed} \rightarrow \text{twin} \rightarrow \text{single domain variant}$$

for a stress-free state, whereas for a clamped condition the evolution sequence is

$$c \rightarrow \text{tweed} \rightarrow \text{twin}$$

To understand the different sequence of morphological evolution under different conditions, let us consider different terms contributing to the elastic energy. From definition it can be seen that E_1 increases with the increase of volume fraction of t'-phase during the $c \rightarrow t'$ transition and is almost a constant after the transformation. This term increases the total free energy of the system during the phase transformation and can significantly shift the equilibrium phase diagram. As a result, the two-phase region of the phase diagram is suppressed. However, it has little effect on the morphology evolution.
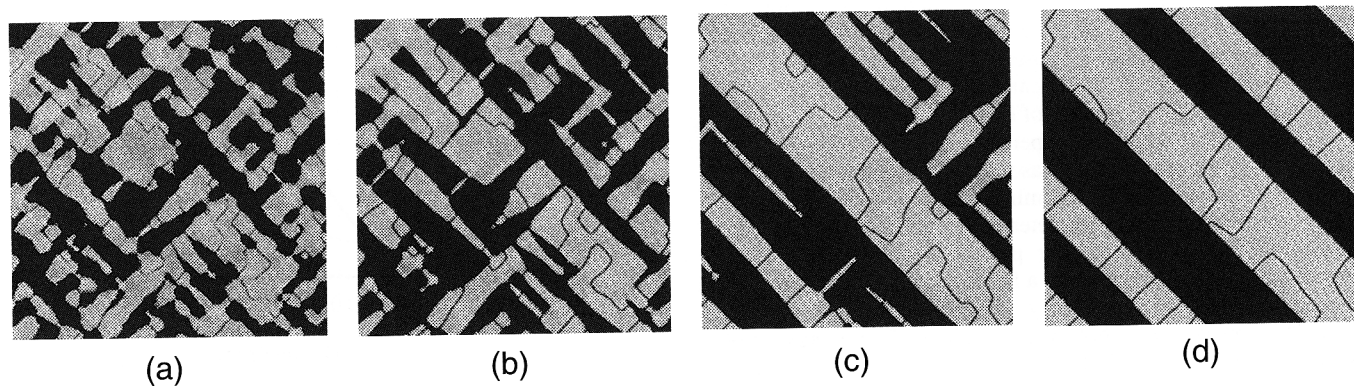
Fig. 4. (a–d) Temporal evolution of $\eta_1(\mathbf{r})$ orientation field during a phase transformation with the total elastic energy $E = E^{het}$. (a–d) correspond to $t^* = 0.2, 1.0, 2.0,$ and 4.0, respectively.
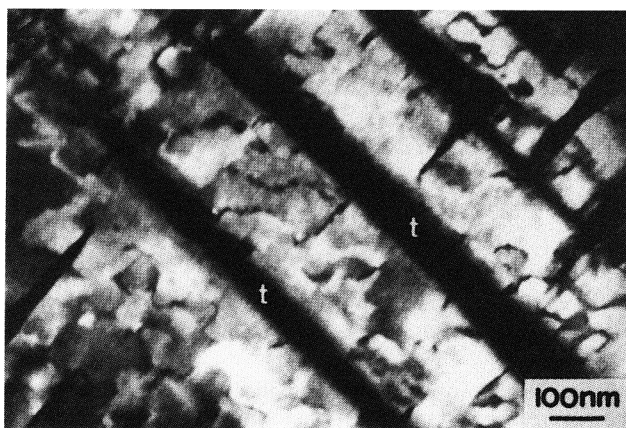
Fig. 5 Twin structure in as-quenched ZrO_2–4 mol% Y_2O_3 alloy (courtesy of M. Doi and T. Miyazaki, see Ref. 4).

The homogeneous strain relaxation energy E^{hom} is dependent on the uniform macroscopic strain $\bar{\varepsilon}_{ij}$ that determines the macroscopic shape deformation of the crystal produced by internal stress due to the second phase. Since this term is approximately proportional to the square of volume fraction of second-phase particles, it makes the phase diagram depend on the volume fraction of second phases. It is intuitively obvious that if the internal strains can be relaxed by shape deformation of the whole system, a single domain has the minimum elastic energy. Hence, it is the E^{hom} term that favors the formation of a single domain. However, if a system is clamped, the homogeneous strain relaxation is not allowed. The final equilibrium structure is then a twin structure made up of different orientation variants.

The heterogeneous relaxation energy E^{het} is dependent on the heterogeneous strain $\delta\varepsilon_{ij}(\mathbf{r})$ which is related to local displacements and does not affect the macroscopic crystal shape. Hence, this term determines the local morphologies of microstructures to minimize the internal strain energy. It is this term which favors the formation of tweed and twin structure during the c–t′ phase transformation.

When a system relaxes to equilibrium, the total nonequilibrium free energy F ($F = F_c + E$) always decreases with simulation time, whereas the elastic energy behaves differently. The dependence of the total elastic energy on the simulation time is shown in Fig. 6. It can be seen that, in the stress-free state, the elastic energy increases during the transformation, then decreases because of the formation of tweed and twin structure, and finally it is reduced to zero for a single domain. Since we include only the heterogeneous strain relaxation term for the elastic energy in the clamped case, the total elastic energy decreases continuously because the elastic relaxation is a spon-
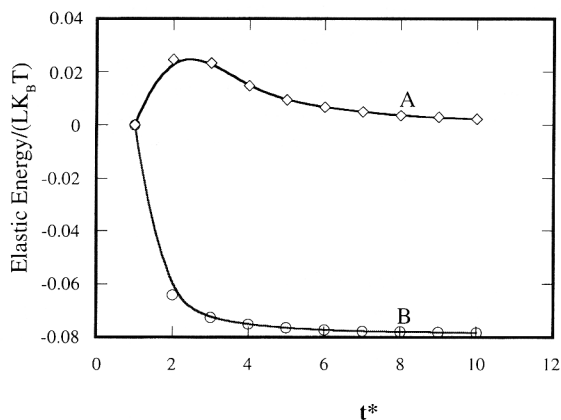
taneous process. This result is consistent with the previous analysis. If the E_1 term was included in the clamped case, the total elastic energy would also increase initially and then later decrease to a certain value due to the heterogeneous strain relaxation.

VII. Summary

The temporal microstructure evolution during the displacive cubic-to-tetragonal ($c → t′$) phase transformation was successfully modeled by employing the time-dependent Ginzburg–Landau equations. The influence of thermodynamic conditions, clamped or stress-free, on microstructure evolution is discussed by analyzing various terms in Khachaturyan's elastic theory for arbitrary distribution of second-phase precipitates reformulated in terms of the diffuse interface theory. Our computer simulation shows that, in the stress-free state, a cubic phase transforms to a single-domain $t′$-phase through intermediate tweed and twin structures, whereas in the clamped condition, the twin structure is stable.

References
[1](a) A. H. Heuer, R. Chaim, and V. Lanteri, "Review: Phase Transformation and Microstructural Characterization of Alloys in the System Y_2O_3–ZrO_2"; pp. 3–20 in Advances in Ceramics, Vol. 24, *Science and Technology of Zirconia III*. Edited by S. Somiya, N. Yamamoto, and H. Yanagida. American Ceramic Society, Westerville, OH, 1988; (b) "The Displacive Cubic → Tetragonal Transformation in ZrO_2 Alloys," *Acta Metall.*, **35** [3] 661 (1987).
[2]V. Lanteri, T. E. Mitchell, and A. H. Heuer, "Morphology of Tetragonal Precipitates in Partially Stabilized ZrO_2," *J. Am. Ceram. Soc.*, **70**, 564 (1986).
[3]V. Lanteri, A. H. Heuer, and T. E. Mitchell, "The Tetragonal Phase in the System ZrO_2–Y_2O_3"; pp. 118–30 in Advances in Ceramics, Vol. 12, *Science and Technology of Zirconia II*. Edited by N. Claussen, M. Rühle, and A. H. Heuer. American Ceramic Society, Columbus, OH, 1984.
[4]M. Doi and T. Miyazaki, "On the Spinodal Decomposition in Zirconia–Yttria (ZrO_2–Y_2O_3) Alloys," *Philos. Mag. B*, **68**, 305 (1993).
[5](a) J. W. Cahn, "On Spinodal Decomposition," *Acta Metall.*, **9**, 795 (1961); (b) "On Spinodal Decomposition in Cubic Crystal," *Acta Metall.*, **10**, 179 (1962).
[6]A. Onuki, "Ginzburg–Landau Approach to Elastic Effects in the Phase Separation of Solids," *Phys. Soc. Jpn.*, **58**, 3065 (1989).
[7]Y. Wang, L. Q. Chen, and A. G. Khachaturyan, "Kinetics of Strain-Induced Morphological Transformation in Cubic Alloys with a Miscibility Gap," *Acta Metall. Mater.*, **41**, 279 (1993).
[8]L. Q. Chen, Y. Z. Wang, and A. G. Khachaturyan, "Transformation-Induced Elastic Strain Effect on the Precipitation Kinetics of Ordered Intermetallics," *Philos. Mag. Lett.*, **64**, 241 (1991).
[9]P. W. Voorhees, G. B. McFadden, and W. C. Johnson, "On the Morphological Development of Second-Phase Particles in Elastically-Stressed Solids," *Acta Metall. Mater.*, **40**, 2979 (1992).
[10]W. C. Johnson and P. W. Voorhees, "Elastically-Induced Precipitate Shape Transitions in Coherent Solids," *Solid State Phenom.*, **23**, 87 (1992).
[11]Y. Wang, H. Wang, L.-Q. Chen, and A. G. Khachaturyan, "Shape Evolution of a Coherent Tetragonal Precipitate in Partially Stabilized Cubic ZrO_2: A Computer Simulation," *J. Am. Ceram. Soc.*, **76**, 3029 (1993).
[12]M. E. Thompson, C. S. Su, and P. W. Voorhees, "The Equilibrium Shape of a Misfitting Precipitate," *Acta Metall. Mater.*, **42**, 2107 (1994).
[13]L. Q. Chen, Y. Z. Wang, and A. G. Khachaturyan, "Kinetics of Tweed and Twin Formation during an Ordering Transition in a Substitutional Solid Solution," *Philos. Mag. Lett.*, **65**, 15 (1992).
[14]S. Semenovskaya and A. G. Khachaturyan, "Kinetics of Strain-Related Morphology Transformation in $YBa_2Cu_3O_{7-δ}$," *Phys. Rev. Lett.*, **67**, 2223 (1991).
[15]K. Parlinski, E. K. H. Salje, and V. Heine, "Annealing of Tweed Microstructure in High T_c Superconductors Studied by a Computer Simulation," *Acta Metall. Mater.*, **41**, 839 (1993).
[16]A. G. Khachaturyan and G. A. Shatalov, "Elastic-Interaction Potential of Defects in a Crystal," *Sov. Phys.—Solid State (Engl. Transl.)*, **11**, 118 (1969).
[17](a) A. G. Khachaturyan, "Some Questions Concerning the Theory of Phase Transformation in Solid," *Sov. Phys.—Solid State (Engl. Transl.)*, **8**, 2163 (1967); (b) see also the monograph *Theory of Structural Transformations in Solid*; pp. 198–212. Wiley, New York, 1983.
[18]J. W. Cahn and J. E. Hilliard, "Free Energy of a Nonuniform System. I. Interfacial Free Energy," *J. Chem. Phys.*, **28**, 258 (1958).
[19]S. M. Allen and J. W. Cahn, "A Microscopic Theory for Antiphase Boundary Motion and Its Application to Antiphase Domain Coarsening," *Acta Metall.*, **27**, 1085 (1979).
[20]J. D. Gunton, M. S. Miguel, and P. S. Sahni, "The Dynamics of First-Order Phase Transitions"; pp. 267–466 in *Phase Transitions and Critical Phenomena*, Vol. 8. Edited by C. Domb and J. L. Lebowitz. Academic Press, New York, 1983.
[21]H. M. Kandil, J. D. Greiner, and J. F. Smith, "Single-Crystal Elastic Constants of Yttria-Stabilized Zirconia in the Range 20° to 700°C," *J. Am. Ceram. Soc.*, **67**, 341 (1981).   □

Fig. 6.   The time dependence of elastic energy during a phase transformation. Curve A: $E = E_1 + E^{hom} + E^{het}$ for the stress-free case; curve B: $E = E^{het}$ for the clamped case; t^* is reduced time.